CONVENTIONAL AND SUPERCONDUCTING RF LINAC DESIGNS FOR THE APT PROJECT

G. Lawrence, D. Barlow, J. Billen, B. Blind, K.C.D. Chan, R. Garnett, R. Gentzlinger, E. Gray, D. Gurd, F. Krawcyzk,
M. Lynch, S. Nath, A. Regan, D. Rees, A. Rohlev, B. Rusnak, R. Ryne, J.D. Schneider, D. Schrage, R. Shafer, J. Sherman,
J. Stovall, H. Takeda, P. Tallerico, T. Wangler, R. Wood, and L. Young
Los Alamos National Laboratory,
Los Alamos, NM 87544, USA

Abstract

The proton linac for the APT (Accelerator Production of Tritium) project will produce a nominal CW beam power of 130 MW at 1300 MeV. Two designs are currently under consideration. The reference design is composed entirely of normal-conducting (NC) copper accelerating structures, while an advanced-technology design employs superconducting (SC) niobium cavities above 217 MeV. The front-end accelerator for both concepts is a 100-mA NC linac. In this paper, the two APT linac designs are described and compared in terms of key factors, including power efficiency, beam loss control, machine availability and flexibility, and construction and operating costs.

Introduction

The overall design of the APT linac, which has a very high beam power, is driven strongly by the large amount of rf power required. Efficient conversion is needed at each stage in the power train to minimize system capital and operating costs. The selection range for basic accelerator parameters [1] (current, energy, accelerating gradient) is determined by the plant production capacity, using a cost-performance model that is based on the energy-dependence of spallation neutron production in high-Z targets, and which includes unit cost estimates for major components and consumables (electricity). Superimposed on this model are technical constraints, including injector current limits and the relationships between peak current, frequency, and beam emittance in low-beta structures.

Normal-Conducting Linac Design

The reference APT linac design is based on copper water-cooled accelerating cavities, and has evolved significantly since it was first presented [2-4]. The NC linac architecture is illustrated in Fig. 1, with additional parameters listed in Table 1. A 75-keV injector housing a microwave-driven ion source [5] generates a continuous 110-mA proton beam. From this input, a 350-MHz, 8-m-long RFQ produces a CW 100-mA beam at 6.7 MeV. The RFQ is built in four segments that are resonantly coupled. RF drive is provided by three 1.2-MW CW klystrons through 250-kW windows.

The RFQ output beam is matched into a 700-MHz CCDTL that accelerates it to 100 MeV. The CCDTL [6] is made up of short sequences of 2-gap and 3-gap accelerating structures embedded within a FODO focusing lattice; quadrupoles are external. Acceleration to the final energy of 1300 MeV is in a 700-MHz side-coupled $\pi/2$-mode linac that continues the same (8-π) focusing period. Fig.2. shows the transition between CCDTL and CCL. The average accelerating gradient (E_0T) is ramped up in the CCDTL and in the first 55 MeV of the CCL to reach 1.3 MV/m, and is held constant thereafter. In general,

the linac accelerating and focusing parameters change very smoothly as beta increases [7].
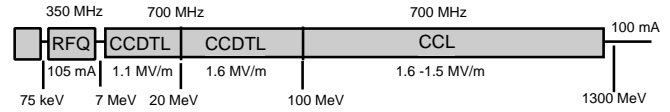

Fig. 1. Architecture of normal-conducting linac design.

Table 1. NC Linac Parameters

Parameter	RFQ	CCDTL	CCL
Structure gradient (MV/m)	1.38	1.10-1.57	1.57-1.49
Avg. gradient (MV/m)	1.38	0.41-1.18	1.18-1.30
Length (m)	8.0	113.0	1166.3
Synchronous phase (deg)	-90 to -60	-60 to -30	-30
Avg. shunt. impedance (MΩ/m)	–	18-33	33-47
Phase adv./period (deg)	–	80	80-35
Quadrupole lattice period		8	8
No. of quadrupoles	–	234	826
Quadrupole gradient (T/m)		87.5	87.5
Trans. emittance (π mm-mrad)*	0.22	0.23	0.23
Long. emittance (π deg-MeV)*	0.214	0.450	0.482
Aperture radius (cm)	0.23-0.34	1.0-1.75	1.75-2.50
Aperture-radius/rms-beam-size	–	5-13	13-26
Copper power losses (MW)	1.26	5.0	54.9
Number of klystrons	3	21	249

* Normalized rms values.

The result is an accelerator design that has strong focusing at low beam energy and is free from phase-space transitions after the RFQ. Beam dynamics analyses and simulations [8,9] have shown these factors to be important in terms of minimizing core emittance growth and the growth of beam halo. As shown in Table 1, the transverse emittance growth is negligible after 20 MeV and longitudinal emittance grows only slightly.
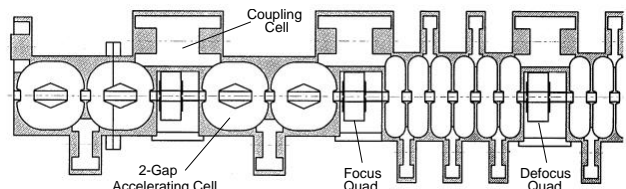

Fig. 2. Transition from CCDTL structure to CCL at 100 MeV

Another design feature is that the cavity and quadrupole aperture dimension increases in steps to 5 cm in the high-energy part of the linac, while the rms beam size shrinks gradually. Fig. 3 shows the dependence of these parameters on beam energy. Also plotted is the transverse position of the proton furthest from the beam core in a typical 100,000 particle simulation. At full energy, the aperture ratio (aper-

ture-to-rms-beam-size) is 25, and at 100 MeV it is 13. The average gradient of 1.3 MV/m in the CCL is high enough to allow a relatively short linac, without producing excessive rf power losses in the copper cavities. Total cavity wall losses in the CCDTL and CCL are 5.0 MW and 54.9 MW respectively. Power deposition per unit length in the CCL is 50-60 kW/m. Both the CCDTL and CCL are driven by 1-MW 700-MHz klystrons through 250-kW windows (tested to > 500 kW).
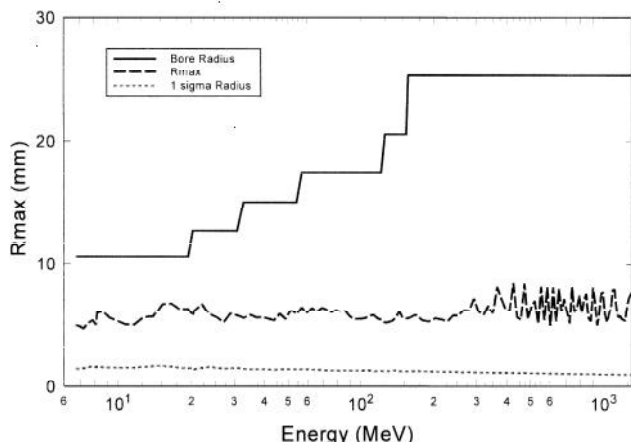

Fig. 3.   Aperture radius, rms beam size, radius of outermost particle.

In order to meet the high availability goal for the APT linac (> 85%), a redundancy scheme is employed for the rf stations, using the accelerating structure itself as a power combiner. The linac is sectioned into "supermodules", each consisting of 100-150 side-coupled accelerating cells, and each provided with n+1 klystrons (typically 5 to 7), where only n units are needed for operation. When an rf station fails, it is isolated by a waveguide switch, and the supermodule continues to provide the full energy gain needed in that section.

Assuming an average plant availability of 75%, the reference APT linac is capable of producing tritium at the rate of 2 kg/yr, with a target design that includes a 10% performance margin. Therefore, the beam power needed to increase plant production capacity to 3 kg/yr (with zero margin) is 174 MW at 1300 MeV. The upgrade path would be to increase the proton current to 134 mA, which would be accomplished by adding a second low energy linac and funneling the two 350-MHz beams at 20 MeV [10]. About 1/3 more rf stations would be added in the high-energy part of the linac to provide the increased beam power.

Superconducting RF Linac Design

A superconducting rf (SC) linac made up of niobium cavities is currently being evaluated as a replacement for the high-energy portion of the APT linac. A feasibility study [11] showed that a SC high-energy linac would reduce the plant electric power demand by 20-25%, and could also offer important technical and operational advantages, including lower beam loss, current/energy flexibility, and improved availability. Fig.4 shows the architecture for a hybrid SC/NC accelerator design now being developed for the APT project. It consists of a 100-mA NC linac injecting into a SC linac at an energy of 217 MeV. Output energy of the SC linac is 1300 MeV for 2-kg/yr production. The low-energy linac is nearly identical to the front end of the reference NC linac described

earlier. The SC linac is composed of cryomodules that contain three or four 5-cell 700-MHz accelerating cavi-ties, alternating with SC quadrupoles in a FODO focusing lattice. There are two kinds of cryomodules; each designed for efficient acceleration in a different energy/velocity range. Cavities in the medium-energy section (from 217 MeV to 469 MeV) are optimized at = 0.64, and in the high-energy sec-tion at = 0.82. Cavity shapes are modeled on the well-established elliptical designs for electron machines, but are compressed along the longitudinal axis in proportion to beta.
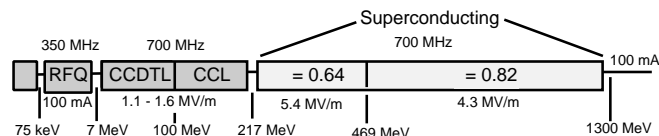

Fig. 4.   Architecture of SC/NC hybrid linac design.

Fig. 5 shows a =0.82 cryomodule, which holds four 5-cell cavities, and five quads. Each cavity is fed by two coaxial rf power couplers, and each cavity pair is supplied by a single 1-MW klystron. The magnets have SC coils and iron poles, and are similar in design to the RHIC trim quads. The medium-beta (=0.64) cryomodules contain three 5-cell cavities, which are powered by one 1-MW klystron, and four quads. Because of the short independently-driven cavities, each section of the SC linac has a very broad velocity bandwidth, which allows the gradient profile of the linac and its output energy to be adjusted over a wide range. About 5% of the accelerating cavities and rf stations are in an operational reserve distributed along the linac to compensate for failed units.
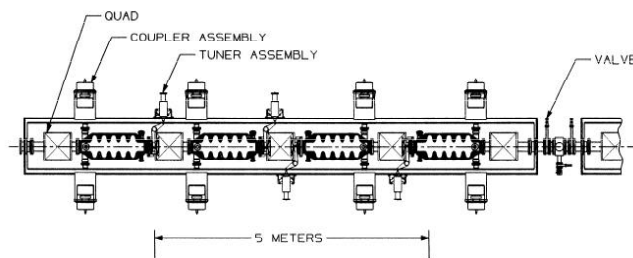

Fig. 5.   High-beta cryomodule (= 0.82) for SC linac.

The production upgrade to 3 kg/yr for the SC linac is to raise the gradient in the high-beta section, increasing the beam energy to 1700 MeV and increasing the beam power to 170 MW. Initial structure gradients for this section have been set at a rather low value (4.1 MV/m), so that a 50% increase can be accommodated at the higher production level.

Because of the high beam current in the APT linac, a major design issue is the power coupler capability. Adjustable antenna-type coaxial couplers are envisioned, with rf windows in the warm region. Since coupler performance with beam has been demonstrated at about 150 kW, and the technology is advancing rapidly, an initial rating of 140 kW per coupler has been specified, with an upgrade to 210 kW in the high-beta section for operation at 3 kg/yr. Table 2. lists key parameters of the two sections of the SC linac (=0.64, =0.82), as well as the last section of the NC linac (100-217 MeV CCL).

The SC-cavity linac can have much larger apertures than the NC linac without incurring significant power penalties. Initial beam simulations show that emittance values are

somewhat larger than in the NC linac, but the resulting aperture ratios are nevertheless much greater, ranging from 35 (at 217 MeV) to 45 (at 1300 MeV).

Table 2. SC Linac Parameters

Parameter	CCL*	β=0.64	β=0.82
Structure gradient (MV/m)	1.57-1.49	5.5	4.1(6.4)
Avg. gradient (MV/m)	1.18-1.30	1.54	1.26(1.89)
Peak surface field (MV/m)	–	19.1	12.7(19.1)
Section length (m)	100.7	204	792
No. of (5-cell) SC cavities	–	90	312
No. of klystrons (1-MW)	34	30	156
Synchronous phase (deg)	-30	-38 to -35	-29
Coupler power (kW)	–	140	140 (210)
Power per klystron (kW)	850	840	560 (840)
Trans. phase adv./period (deg)	80-35	81.5-66.7	81.2-79.0
Quadrupole length (cm)	5.4	30.5	45.9
No. of quadrupoles	125	120	390
Quadrupole gradient (T/m)	87.5	6.4-8.1	5.4 - 12.6
Trans. emittance (mm-mrad)	0.23-0.29	0.29	0.33
Long. emittance (deg-MeV)	0.5	0.5	0.8
Aperture radius (cm)	1.75-2.5	6.5	8.0
Aperture-radius/rms-beam-size	13-17	35	45
Thermal load @ 1.9K (kW)	–	2.0	6.1 (9.2)

* 100-217 MeV section. Numbers in parentheses are for 3-kg/yr,

Design Issues and Comparisons

The NC and SC linac point designs developed for APT have matured to the point that comparisons can be made with respect to major criteria, including 1) construction and operating cost, 2) power efficiency, 3) beam loss, 4) availability, and 5) operational flexibility.

Preliminary estimates show that construction costs would be similar, with a modest (5-10%) advantage to the SC linac. Greater unit costs for the accelerating structures are offset by the smaller rf power installation. Refrigeration system costs are nearly balanced by reduced water cooling system costs. Annual operating costs for a SC-based APT plant will be significantly lower (15%) than for a NC-based plant due to reduced electric power requirements.

Electrical efficiency of the SC linac design is clearly greater than the NC design, (0.40 vs 0.33) because 48 MW of cavity rf losses are eliminated. The 8 MW needed to run the cryoplant is offset by reduced water-cooling pumping power and elimination of quadrupole magnet power in the SC linac.

The aperture ratio is much greater in the SC linac than in the NC linac, greatly reducing halo interception, and dramatically relaxing alignment and steering requirements. In terms of activation threat to the accelerator, the transition to a large aperture at about 200 MeV is advantageous, since neutron production rises rapidly in this energy region.

The major source of unavailability for either of the linac designs lies in the large number of rf power stations and their critical components (klystrons, power supplies, etc). In the NC linac, the supermodule architecture provides rf station redundancy for each 25-MeV segment of the linac, allowing failures to occur without interrupting operation for more than a few minutes. In the SC linac, high availability is provided by the 5% reserve cavities and klystrons. After a failure, one of the reserve units is energized, and phases and amplitudes of

the downstream linac are reset to maintain an optimum acceleration profile. Small changes in output energy that may result after retuning are tolerable because of the wide momentum acceptance of the HEBT and target system.

In the NC linac, the accelerating gradient and maximum beam energy are fixed by the beta profile of the long coupled chains of cavities, although operation at reduced energies is possible by turning off the highest-energy rf stations. In the SC linac, operational flexibility is enhanced by the retunability of the accelerator and the adjustability of the cavity gradients. It is practical to increase proton energy to compensate for reduced current to provide a given beam power. In both designs, electrical efficiency is highest when using the full output capacity of the klystrons, so schemes for power-grid load leveling would be best implemented by turning off the final section of the linac.

We believe that either linac design is a practical approach to APT, but the SC linac would be superior in terms of operating cost, beam loss, availability risk, and operational flexibility. With respect to ED&D (engineering development and demonstration), the LEDA program [12] is prototyping the low-energy linac at full CW power. The high-energy NC linac needs little further ED&D. For the SC linac, cavity prototyping is needed, since the medium-beta cavity shapes differ from the (=1) shapes used for electron accelerators. Confirmation of insensitivity to proton irradiation is another task. Finally, complete pre-production prototypes of the SC cryomodules must to be built and tested; these are structurally different than existing units at CEBAF, CERN, DESY and KEK, because of the high density of quadrupole magnets. Programs to provide the needed tests and demonstrations are underway.

References

[1] G.P. Lawrence, "Critical Design Issues of High-Intensity Proton Linacs", Proc. 1994 European Particle Accelerator Conference, EPAC94, London, 236 (June, 1994).
[2] T.P. Wangler, et al., "Linear Accelerator for Production of Tritium: Physics Design Challenges", Proc. 1990 Int. Linac Conf., Albuquerque, NM, 548 (Sept 1990).
[3] J.H. Billen et al., "A Versatile High-Power Linac for Accelerator-Driven Transmutation Technologies, Proc. 1995 Particle Accelerator Conf., Dallas, IEEE No. 95CH35843, 1137 (1995).
[4] S. Nath et al., "Physics Design of APT Linac with Normal Conducting rf Cavities," Proc. 1996 Int. Linac Conf., Geneva, Aug 1996.
[5] J.D. Sherman et al., "Development of a 110-mA 75-keV Proton Injector for High-Current CW Linacs," Proc. 1996 Int. Linac Conf., Geneva (Aug 1996).
[6] J.H. Billen et al., "A New RF Structure for Intermediate-Velocity Particles," Proc. 1994 Int. Linac Conf., Tsukuba, p341 (1994).
[7] J.H. Billen, "Smooth Accelerating Strategy for Intense Ion Beams, Advances in Accelerator Structures (Long RFQ, CCDTL)," Proc. 1996 Int. Linac Conf., Geneva (Aug 1996).
[8] R.D. Ryne, "Halos of Intense Proton Beams," Proc. 1995 Particle Accelerator Conf., Dallas, IEEE No. 95CH35843, 3149 (1995).
[9] T.P. Wangler, "Dynamics of Beam Halo in Mismatched Beams," Proc. 1996 Int. Linac Conf., Geneva (Aug 1996).
[10] S. Nath, "Funneling in LANL high intensity Linac Designs," Proc. of 1994 Int. Conf. on Accelerator-Driven Transmutation Technologies and Applications, Las Vegas (July 1994).
[11] K.C.D. Chan, "Conceptual Design of a Superconducting High-Intensity Proton Linac," 1996 Int. Linac Conf., Geneva (Aug 1996).
[12] J. D. Schneider, "APT Accelerator Technology," Proc. of 1996 Linear Accelerator Conf., Geneva, August 26-30, 1996.